

## Supporting Information

### **Probing biotransformation of hematite nanoparticles and magnetite formation mediated by *Shewanella oneidensis* MR-1 at molecular scale**

Hong-Wei Luo<sup>‡</sup>, Xin Zhang<sup>‡</sup>, Jie-Jie Chen, Han-Qing Yu, Guo-Ping Sheng\*

CAS Key Laboratory of Urban Pollutant Conversion, Department of Chemistry,

University of Science and Technology of China, Hefei, 230026, China

<sup>‡</sup> These authors contributed equally to this work

**\* Corresponding author:**

Prof. Guo-Ping Sheng

Fax: +86-551-63601592

E-mail: [gpscheng@ustc.edu.cn](mailto:gpscheng@ustc.edu.cn)

This supporting information contains 8-page document, including 3 tables, 4 figures  
and this cover page.

**Table S1** STXM describing Fe(III) surface density on the surface of hematite NPs as a function of incubation time with *Shewanella oneidensis* MR-1.

| Incubation time (h) | Min surface density ( $\mu\text{g}/\text{cm}^2$ ) | Max surface density ( $\mu\text{g}/\text{cm}^2$ ) |
|---------------------|---|---|
| 24                  | 1.57837e-005                                      | 1.25190e-004                                      |
| 48                  | 1.56226e-005                                      | 1.18898e-004                                      |
| 72                  | 1.04495e-005                                      | 3.13369e-005                                      |
| 144                 | 9.88261e-006                                      | 2.63732e-005                                      |

**Table S2** Raman shifts and assignments of Fe(III) and Fe(II) minerals.

| Raman shift (cm <sup>-1</sup> ) | Assignment               | Fe minerals |
|---------------------------------|--------------------------|-------------|
| 218                             | Fe-O sym. str            | hematite    |
| 289                             | Fe-O sym. bend           | hematite    |
| 403                             | Fe-O sym. bend           | hematite    |
| 491                             | Fe-O sym. str            | hematite    |
| 516                             | Fe-O asym. bend          | magnetite   |
| 600                             | Fe-O sym. bend           | hematite    |
| 658                             | Fe-O sym. str            | magnetite   |
| 968                             | PO <sub>4</sub> sym. str | vivianite   |

**Table S3** Calculated free energy change ( $\Delta G$ ) on the crystal surface of hematite upon microbial reduction.

| Redox reaction equations   | $\Delta G$ (kJ/mol) |
|--|---------------------|
| $[\text{Fe}(\text{OH})(\text{H}_2\text{O})_5]^{2+} + \text{H}_2\text{PO}_4^- + \text{e}^- \rightarrow \text{Fe}(\text{HPO}_4)(\text{H}_2\text{O})_5 + \text{H}_2\text{O}$                    | -356.352            |
| $[\text{Fe}(\text{OH})_2(\text{H}_2\text{O})_4]^+ + 2\text{H}_2\text{PO}_4^- + \text{e}^- \rightarrow [\text{Fe}(\text{HPO}_4)_2(\text{H}_2\text{O})_4]^{2-} + 2\text{H}_2\text{O}$          | -124.220            |
| $\text{Fe}(\text{OH})_3(\text{H}_2\text{O})_3 + 3\text{H}_2\text{PO}_4^- + \text{e}^- \rightarrow [\text{Fe}(\text{HPO}_4)_3(\text{H}_2\text{O})_3]^{4-} + 3\text{H}_2\text{O}$              | 258.200             |
| $[\text{Fe}_2(\text{OH})_4(\text{H}_2\text{O})_6]^{2+} + \text{H}_2\text{PO}_4^- + \text{e}^- \rightarrow \text{Fe}_2(\text{HPO}_4)(\text{OH})_3(\text{H}_2\text{O})_6 + \text{H}_2\text{O}$ | -340.164            |
| $[\text{Fe}_2(\text{OH})_4(\text{H}_2\text{O})_6]^{2+} + \text{H}_2\text{PO}_4^- + \text{e}^- \rightarrow \text{Fe}_2(\text{PO}_4)(\text{OH})_2(\text{H}_2\text{O})_6 + 2\text{H}_2\text{O}$ | 47611.193           |

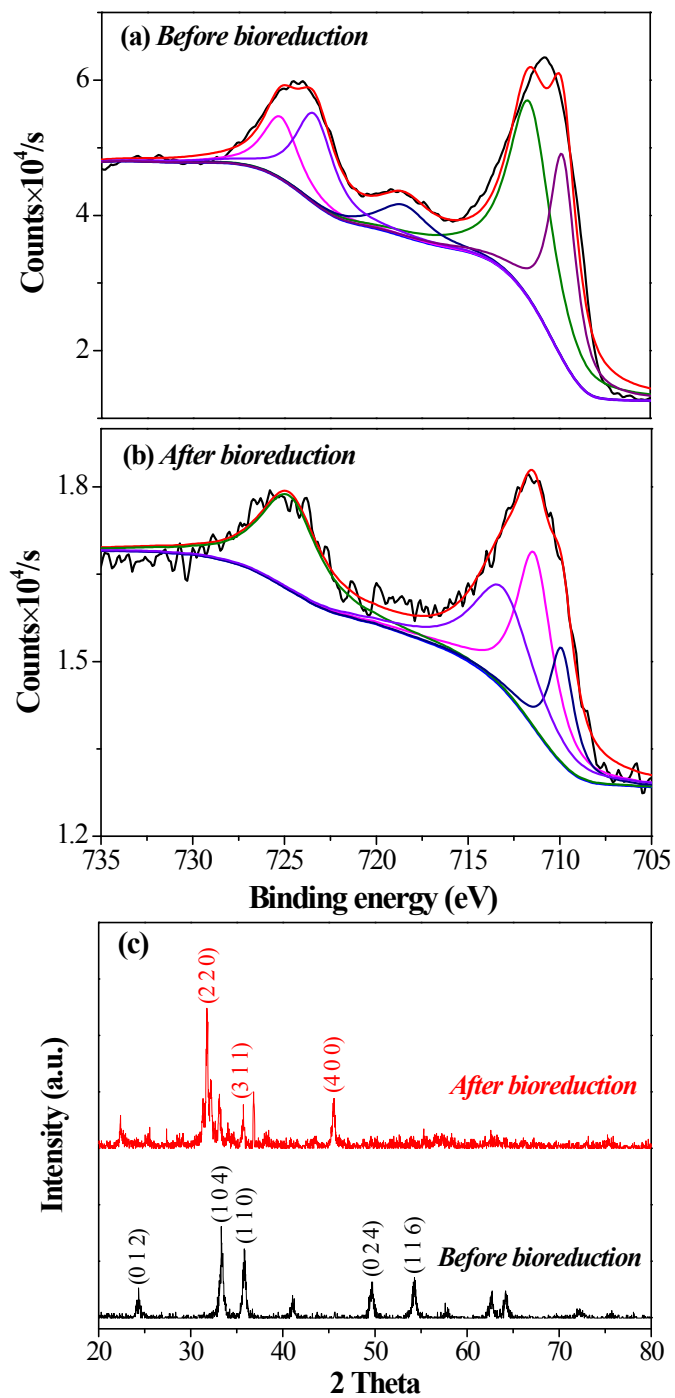


**Figure S1.** High-resolution XPS spectra showing the Fe2p region (a, b); and XRD patterns (c) before and after bioreduction of hematite NPs (50 ppm) for 48 h.

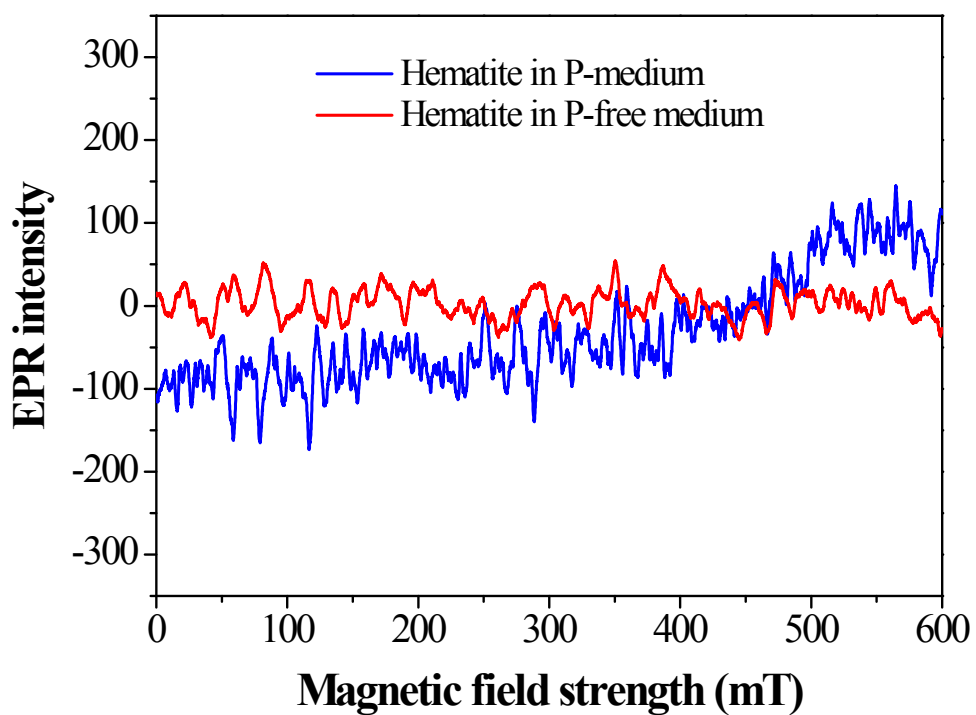


**Figure S2.** EPR spectra of hematite NPs (100 ppm) exposed to sterile medium with and without phosphate.

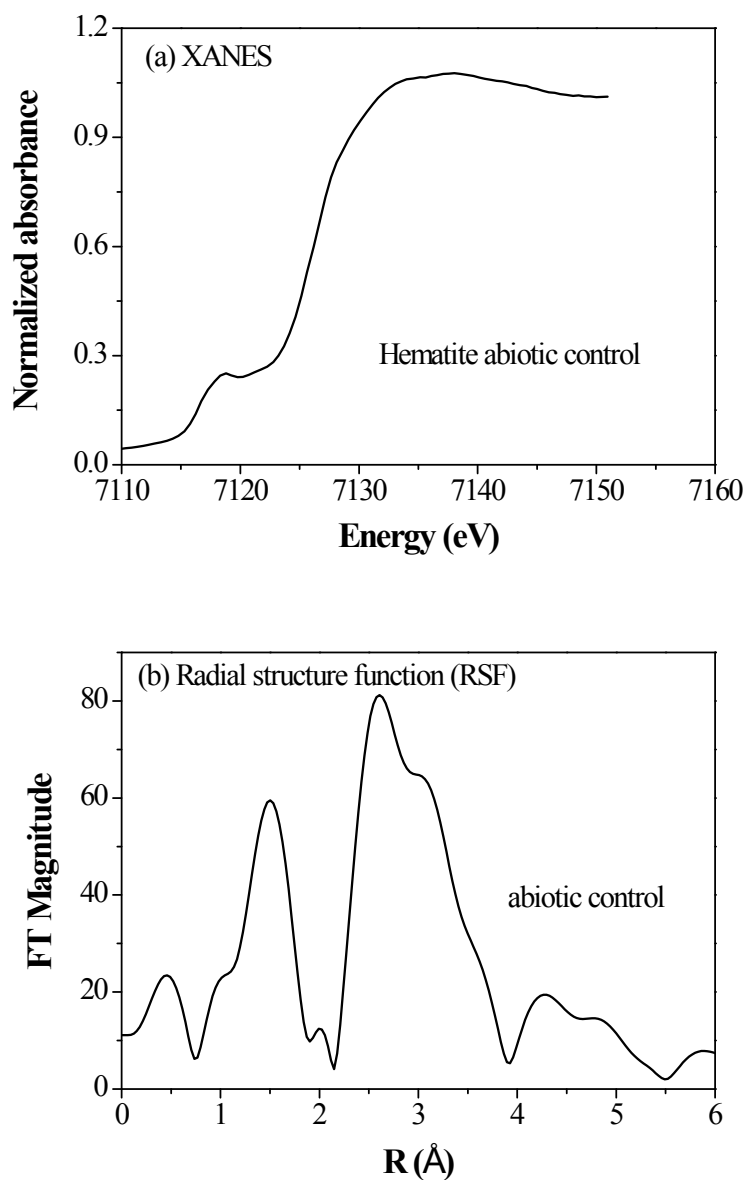


**Figure S3.** (a) Fe K-edge XANES spectra of hematite (100 ppm) in abiotic control; and (b) the corresponding radial structure function (RSF) derived from Fourier transformations.

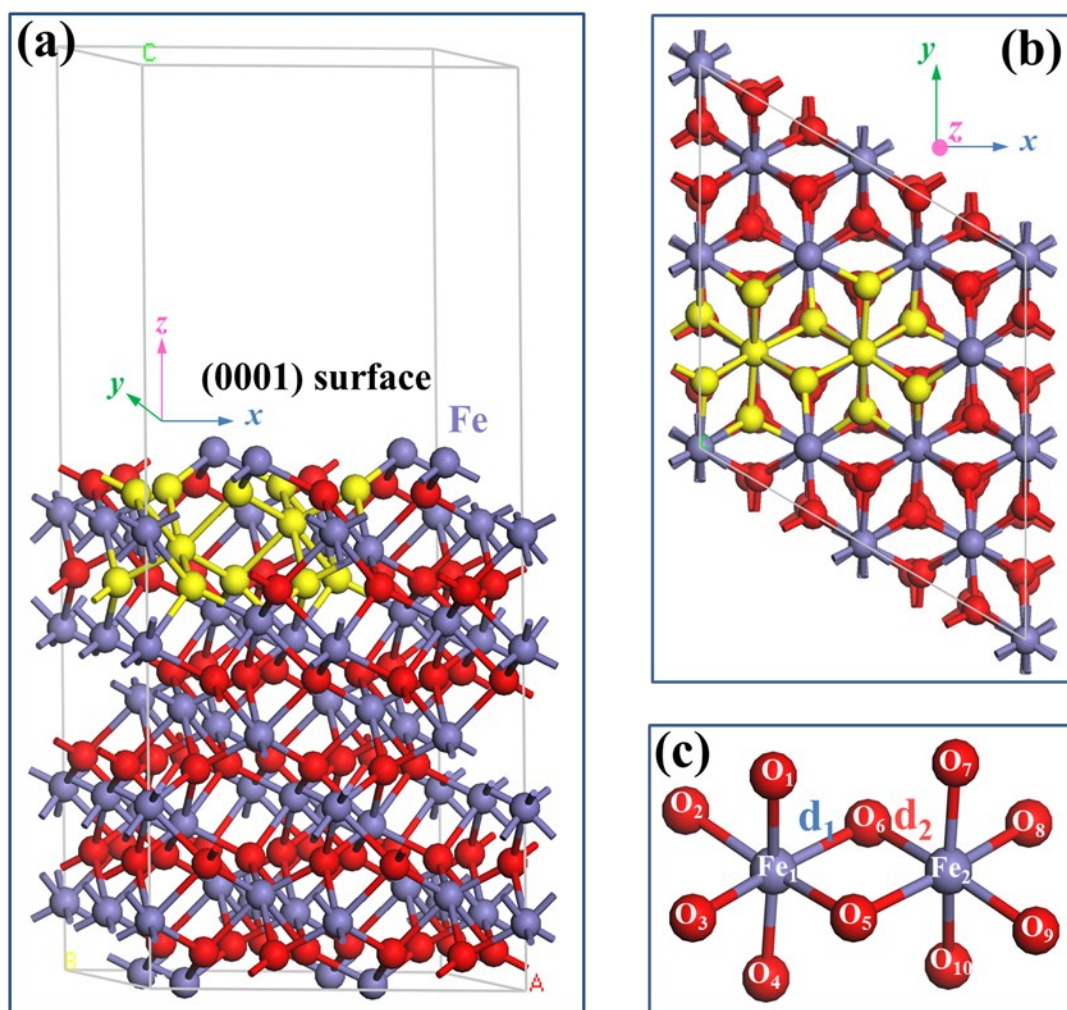


**Figure S4.** Structural characteristics of  $\alpha$ - $\text{Fe}_2\text{O}_3$ . (a) (0001) crystal surface of  $\alpha$ - $\text{Fe}_2\text{O}_3$  with (2 $\times$ 2) supercell ( $a = b = 10.076 \text{ \AA}$ ,  $c = 23.167 \text{ \AA}$ ,  $\alpha = \beta = 90^\circ$ ,  $\gamma = 120^\circ$ ); (b) the top view of the (0001) crystal surface with the unit monodentate and bidentate oxygen ligands highlighted; and (c) the structure of bidentate oxygen ligands on the (0001) crystal surface of  $\alpha$ - $\text{Fe}_2\text{O}_3$  with two types of Fe-O distances:  $d_1 = 1.946 \text{ \AA}$ , and  $d_2 = 2.116 \text{ \AA}$ ,  $\text{Fe}_1\text{-O}_2$ ,  $\text{Fe}_1\text{-O}_4$ ,  $\text{Fe}_1\text{-O}_6$ ,  $\text{Fe}_2\text{-O}_5$ ,  $\text{Fe}_2\text{-O}_7$ , and  $\text{Fe}_2\text{-O}_9$  equal  $d_1$ , and  $\text{Fe}_1\text{-O}_1$ ,  $\text{Fe}_1\text{-O}_3$ ,  $\text{Fe}_1\text{-O}_5$ ,  $\text{Fe}_2\text{-O}_6$ ,  $\text{Fe}_2\text{-O}_8$ , and  $\text{Fe}_2\text{-O}_{10}$  equal  $d_2$ .